Appl Microbiol Biotechnol (2013) 97:3593–3601
DOI 10.1007/s00253-012-4603-1

Evaluation of anti-quorum sensing activity of silver nanowires

Mohini S. Wagh (nee Jagtap) · Rajendra H. Patil · Deepali K. Thombre · Milind V. Kulkarni · Wasudev N. Gade · Bharat B. Kale

Received: 12 September 2012 / Revised: 13 October 2012 / Accepted: 17 November 2012 / Published online: 8 December 2012

Abstract A menace of antimicrobial resistance with growing difficulties in eradicating clinical pathogens owing to the biofilm has prompted us to take up a facile aqueous-phase approach for the synthesis of silver nanowires (SNWs) by using ethylene glycol as a reducing agent and polyvinylpyrrolidone (PVP) as a capping agent. This synthesis is a reflux reaction seedless process. The obtained SNWs were about 200–250 nm in diameter and up to 3–4 μm in length. The SNWs were characterized by field emission scanning electron microscopy, transmission electron microscopy, UV–Vis spectroscopy, and X-Ray powder diffraction, and the chemical composition of the sample was examined by energy dispersive X-ray spectrum. The SNWs did not show an antibacterial activity against test organisms, *Bacillus subtilis* NCIM 2063 and *Escherichia coli* NCIM 2931; however, it showed a promising property of a quorum sensing-mediated inhibition of biofilm in *Pseudomonas aeruginosa* NCIM 2948 and violacein synthesis in *Chromobacterium violaceum* ATCC 12472, which is hitherto unattempted, by polyol approach.

Keywords Silver nanowires · Polyol · Anti-quorum · Pseudomonas · CLSM

Introduction

It is well known that silver ions and silver-based compounds are highly toxic to microorganisms (Kim et al. 2007; Rai et al. 2012; Salata 2004), and have been used in various fields of biological applications (Chen and Schluesener 2008). However, as the over/misuse of antibiotics have led to the resurgence of antibiotic resistance in pathogenic microorganisms (Knothe et al. 1987), it is likely that nanoparticle-based therapeutics may give rise to similar resistance, so there is a need to search for an alternative strategy to tackle the growing menace of resistance in pathogenic microorganisms. An important aspect of many pathogenic organisms during their progression in a pathogenic state is a cooperative behavior towards synthesis of the biofilm, in a process called quorum sensing (QS) (Whitehead et al. 2001). The QS is a phenomenon in which bacterial populations coordinate communal behavior through a process of chemical cell-to-cell signaling mediated by diffusible signal molecules (Reading and Sperandio 2006; Suman et al. 2009). QS has been known to control a wide array of phenotypes in bacteria ranging from simple bacterial cell motility to complex communal behaviors such as biofilm formation and production of virulence factors (Davies 2003). The biofilms formed by bacterial communities in aqueous conditions have been shown to contaminate a wide variety of infrastructures, such as plumbing, oil refineries, paper mills, heat exchangers, and medical implant systems (Banerjee et al. 2011). And in medical settings, biofilms are the cause of persistent infections, often endangering the functionality of the indwelling catheters. Moreover, biofilms have been estimated to cause 80 % or more of all microbial infections in humans (Davies 2003). Since biofilms protect their constituent cells in various ways, it becomes increasingly difficult to treat clinical and industrial contamination (Blango and Mulvey 2009). Also, the cooperative behavior of bacterial cells, mediated by cell–cell communications, enhanced resistance to antimicrobial agents and the host's defenses. A wide range of bacteria-resistant surfaces have been proposed to inhibit biofilm growth (Rana and Matsuura 2010); however, there are only few reports on the use of nanostructures as an antibiofilm agent (Lellouche et al. 2009).

M. S. Wagh (nee Jagtap) · M. V. Kulkarni (✉) · B. B. Kale
Nanocomposite/Glass Laboratory, Centre for Materials for Electronics Technology (C-MET), Department of Information Technology, Government of India, Panchawati, Off Pashan Road, Pune 411008, India
e-mail: milindcmet@yahoo.com

R. H. Patil · D. K. Thombre · W. N. Gade
Department of Biotechnology, University of Pune, Pune 411007, India

Nanostructures have attracted steadily growing interest due to their fascinating properties and intriguing applications that are complementary or superior to those of bulk materials (Xia et al. 2003). The inherent property of nanostructure materials is a large surface-to-bulk ratio. As interesting as spherical metal nanoparticles are, one-dimensional (1-D) metal nanostructures are of even more fundamental and practical interest in recent years (Murphy et al. 2006). These are expected to play important role in fabricating nanoscale devices due to their unique electrical, optical, magnetic, and thermal properties (Zhai et al. 2009). The synthesis of metal nanorods and nanowires of desired size and shape has enormous importance in nanotechnology because of its characteristic shape- and size-dependent optical, electronic and chemical properties.

Metal nanowires with an extremely high aspect ratio are focused due to their excellent electrical, thermal, optical, and/or catalytic properties in combination with their stability for various potential applications such as conducting nanoscale electronic sensing devices, conductive adhesive, surface enhanced Raman scattering, photonic crystals, etc. (Chen et al. 2007; Hu et al. 2010; Hu and Chan 2004; Huang et al. 2001; Murphy et al. 2006). Since, these properties are size-dependent, many physical and chemical approaches have been developed including seed-based synthetic method (Chen and Gao 2004; Sancia and Volkan 2009), electrochemical method (Peppler and Janek 2007), solvothermal route (Chen et al. 2010; You et al. 2009), electrodeposition on templates (Evans et al. 2008), wet chemical method (Caswell et al. 2003; Hu et al. 2004), photochemical method (Zou et al. 2004), sonochemical route (Yang and Li 2008; Zhu et al. 2010), and so on. Though the above-mentioned approaches of physical templates can ensure a good control over the morphology of the final products and thus gain metal nanowires with high aspect ratios, the addition and then the removal of the templates may complicate the synthetic procedures and limit the scale at which a material can be synthesized.

One of the most popular synthesis techniques for the synthesis of silver nanostructures is the polyol method (Fievet et al. 1989). The temperature-dependent reducing power of polyol makes metals ideal for the synthesis of particles over a broad range of sizes by controlling the nucleation and growth processes through careful regulation of reaction temperature (Wiley et al. 2005).

In our earlier study, we report of PANI-Ag (Tamboli et al. 2012) as an excellent antibacterial agent against Gram-positive and Gram-negative organisms. In continuing the antibacterial studies, we have attempted a synthesis of silver nanowires (SNWs) by polyol reduction method in the presence of polyvinylpyrrolidone (PVP) as a capping agent and ethylene glycol as the solvent and reductant, and have studied its application in the field of biology as an agent that inhibits the formation of biofilm in *Pseudomonas aeruginosa* and violacein production in *Chromobacterium violaceum*, both QS-mediated traits. To our knowledge, this is the first report of SNWs as anti-QS agents synthesized by polyol reduction method.

Materials and methods

Synthesis of nanomaterials

The polyol process we have used for the synthesis of SNWs was mainly based on ethylene glycol, which served as a good solvent for both $AgNO_3$ and PVP. In a typical synthesis, a three-necked round-bottom flask (equipped with a condenser, thermo controller, and magnetic stirring bar) containing pure ethylene glycol was refluxed for 1 h at about 160 °C. Then silver nitrate (0.25 M) and PVP (0.375 M) were simultaneously added in refluxing ethylene glycol (EG) solution. After injection, the reaction mixture was continued for reflux at 160 °C for another 45 min. Finally, the reaction was stopped, allowing the product to cool to room temperature. The reaction mixture gradually turned turbid, and a yellow and gray suspension was obtained. During the whole reaction process, the temperature was kept at 150–160 °C. Vigorous magnetic stirring was continuously applied throughout the entire process of reduction and wire growth. The as-obtained product was separated by centrifugation at 3000 rpm for 10 min and then washed with deionized water. The procedure was repeated several times to get a purified product.

The transmission electron microscopy (TEM) images were obtained on a transmission electron microscope (TEHNAI G220) with an accelerating voltage of 80 kV. A drop of the solution-containing samples was put onto copper grids, which was dried at room temperature. The morphologies of the as-prepared samples were studied by field emission scanning electron microscopy (FESEM, Hitachi S4800) at an accelerating voltage of 20 kV. An energy dispersive (ED) detector was equipped with this transmission electron microscope. The X-ray diffraction spectra (XRD) measurements were performed on a Brucker-AXS Model D8 advance instrument by using Cu Kα radiation (50 kV). The XRD patterns were recorded from 10° to 90° with a scanning rate of 0.067°/s. UV/Vis absorption spectra were taken at room temperature on a Perkin-Elmer Lambda 950 Spectrophotometer in the range of 300–900 nm.

The effect of SNW particles on the QS-controlled synthesis of violacein was determined using *C. violaceum*, a wild-type pigment-producing strain, and biofilm formation was determined by using *P. aeruginosa*.

Determination of antibacterial activity

For determining the minimum concentration of SNWs required to inhibit the growth of *Bacillus subtilis* NCIM

2063and *Escherichia coli* NCIM 2931, a modification of broth dilution method was used. This method facilitates the testing of inhibitory activity at various nanoparticle concentrations in Muller Hinton (MH) broth. The MH broth was supplemented with different concentrations of nanoparticles (0.125–4 mg/mL) and inoculated with bacterial suspension to obtain 10^6 colony forming units (CFU)/mL. Control tubes were maintained without SNWs. As SNWs formed a turbid solution in LB broth, instead of observing the turbidity as a measure of minimum inhibitory concentration (MIC) value, counting of the viable number of bacteria (in CFU/milliliter), in comparison to control, was performed.

Violacein synthesis and quantification

C. violaceum ATCC 12472 was cultivated in the presence of SNWs (0.125–4 mg/mL) in Luria–Bertaini (LB) broth and incubated at 30 °C in a shaker for 18 h. One milliliter of culture from each concentration was centrifuged at 13,000 rpm for 10 min to pelletize the cells along with insoluble violacein. The culture supernatant was discarded, and 1 mL of dimethyl sulphoxide (DMSO) was added to the pellets. The solution was vortexed vigorously for 30 s to completely solubilize violacein and was centrifuged at 13,000 rpm for 10 min to remove the cell debris, and the absorbance of violacein content in the DMSO was read at 585 nm in microplate reader (Schimadzu, Japan).

Biofilm formation and quantification

P. aeruginosa NCIM 2948 was grown overnight in LB broth at 37 °C with agitation. After growth, the culture was diluted with LB medium (OD_{600} 0.02), and 50 μl of the diluted culture was added to 940 μl of LB medium supplemented with 0.125–4 mg/mL of SNWs and were incubated statically for 18 h at 37 °C in 24-well polystyrene plates. After incubation, planktonic bacteria present in the media were discarded, and the biofilms were washed three times with phosphate-buffered saline buffer. Washed biofilms were fixed with 1 mL of methanol (99 %). After 15 min, the methanol was discarded, and the plates were dried at room temperature. Crystal violet (0.1 % in water) was then added to each well (1 mL/well), and the plates were incubated for 15 min at room temperature. Crystal violet was then discarded, and stained biofilms were washed three times with 1 mL of water. Acetic acid (33 % in water) was added to the stained biofilms (2 mL) in order to solubilize the crystal violet, and the absorbance of the solution was read at 590 nm (Schimadzu, Japan).

Scanning electron microscopy and confocal scanning laser microscopy of biofilm

Biofilms that formed on polystyrene flat-bottomed microtitre plates in the presence sub-MIC concentrations of SNWs (2 mg/mL) were fixed in 2 % glutaraldehyde in 0.1 M cacodylate buffer (pH 7.5 for 4 h at 4 °C. After thoroughly washing with cocdylate buffer, samples for SEM were dehydrated in a series of ethanol solutions (30–100 %), vacuum-dried, mounted on aluminum stubs with conductive carbon cement, and coated with a gold film. Samples were observed with scanning electron microscope (Joel, Japan). Samples for confocal laser scanning microscopy (CLSM), after thorough washing, were treated with 5-μM fluorescent dye, Concavallin A Alexafluor 488, with an excitation at wavelength of 488 and emission at 520 (Ziess Carl, Germany).

Results

FESEM characterization

The FESEM images of as-synthesized SNWs are shown in Fig. 1a, b. It is observed from the micrographs that there is a formation of uniform-sized silver nanocubes and nanowires. The size of the nanocubes was observed to be ~ 240 nm. The surface of nanowires was relatively uniform with smooth tapering end having an average diameter of ~ 200–250 nm and a length of up to few microns. Diameters of the nanowires were more or less identical.

TEM characterization

A representative TEM image of as-synthesized SNWs is shown in Fig. 2, which supports well to the formation of uniform silver rods observed in the FESEM analysis described above.

XRD characterization

Figure 3 shows XRD pattern of SNWs. It showed that as-synthesized SMWs were highly crystalline. All diffraction peaks could be readily indexed to the (111), (200), (220), and (311) planes of pure face-centered cubic silver (JCPDS File 04-0783), and no impurities were observed. The calculated lattice constant from XRD pattern was 4.0867 Å which is perfectly in agreement with the literature value (4.0867 Å). The energy dispersive X-ray analysis (Fig. 4) of a sample provides further evidence for the SNWs.

Ultraviolet–visible spectrophotometry

Figure 5 shows the UV–visible spectra of the as-prepared SNWs. The centrifuged sample exhibit two surface plasmon resonance peaks; absorption peak at 349 nm can be attributed to the plasmon response of long SNWs (Tian et al. 2009). The shoulder peak at 349 nm was an optical characteristic similar to bulk silver, which is usually been observed

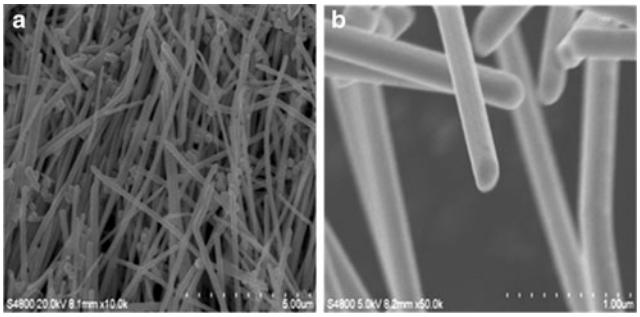

Fig. 1 FESEM images of silver nanowires (**a** and **b**)

for SNWs (Shen et al. 2007; Wang et al. 2005; You et al. 2009). The second peak at 389 nm corresponds to the transverse plasmon band of SNWs. It is well known that two plasmon modes, transverse and longitudinal modes, are expected for 1-D metallic nanostructures.

Antibacterial activity

We have modified the MBC determination method and measured the inhibition by counting the number of viable cells as CFU/milliliter, since SNWs in MH broth gave a white turbid color in MIC tubes. The antibacterial action of the as-synthesized SNWs was as shown in Fig. 6. When the cells of test organisms were subjected to different concentrations of SNWs, no reduction in the number of viable cells was observed. The number of cells in control and test samples after 12–16 h of incubation remained constant, approx. 1×10^8/mL.

Anti-quorum sensing and biofilm

A graphical representation of events of SNWs inhibiting the QS-mediated biofilm formation in *P. aeruginosa* was shown in Fig. 7.

The QS inhibition of violacein biosynthesis in *C. violaceum* and biofilm formation in *P. aeruginosa* was as shown in Figs. 8 and 9, respectively. Based on a modification of previously described method (Martinelli et al. 2004), a spectrophotometric assay was performed to quantify the relative amount of (violacein) pigmentation of wild-type *C. violaceum* in the presence of SNWs. As the pigments from this wild-type strain may absorb light at a wavelength used for monitoring bacterial cell density (540–700 nm), the mutant strain *C. violaceum* CV026—a mutant incapable of producing the pigments—was used for the assessment of the effects of SNWs on the growth of the test organisms. Thus, in this modified assay, the effect on pigment production was assessed in the wild-type strain, while the effect on growth was monitored using the mutant nonpigmented strain. When the cells of *C. violaceum* were incubated with SNWs, there was a decrease in the synthesis of violacein in *C. violaceum* (Fig. 8); this inhibition started at 0.5 mg/mL and continued till 4 mg/mL, after which growth of cells ceased. Compared to 100 % violacein synthesis in the control, at 0.5 mg/mL, there was a reduction of about 60 % of violacein synthesis, while at 4 mg/mL, the reduction was by 80 %.

When *P. aeruginosa* was grown in different concentrations of SNWs, it was found that the highest decrease in the formation of biofilm was at 4 mg/mL, without effecting the growth in comparison to that in the control (Fig. 9). However, at increasing concentration, there was a decrease in the number of viable cells. Therefore, 4 mg/mL of SNWs significantly arrested biofilm formation without affecting viability, whereas concentration above it inhibited the growth of the organism itself. The SEM analysis of the biofilm at 4 mg/mL was as shown in Fig. 10. It can be observed that in the presence of SNWs, the outermost covering of the matrix was aloofed, thus exposing the cells underneath; however, the control sample showed cells with a layer of matrix, a typical of intact biofilm.

To further understand the biofilm inhibition, CLSM was used to study the formation of biofilm in the presence of SNWs. Figure 11 describes the effect of sub-inhibitory concentration of SNWs on biofilm formation ability of *P. aeruginosa*. Under CLSM, the biofilm in the presence of SNWs was seen as fractured green fluorescence with lower intensity, shown as an insert in the figure. However, in the absence of SNWs, the fluorescence intensity was linear and intense, indicating an intact biofilm.

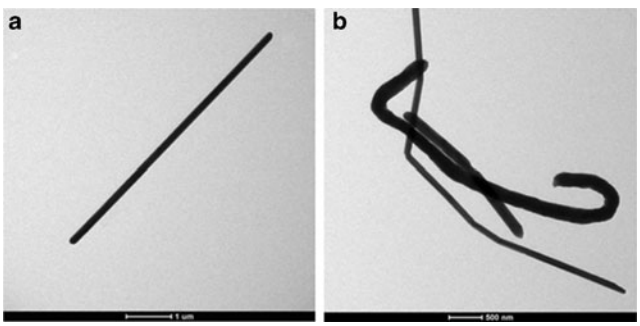

Fig. 2 TEM images of silver nanowires (**a** and **b**)

Discussion

Antibacterial

With the emergence and increase of microbial organisms resistant to multiple antibiotics, and the continuing emphasis on health-care costs, many researchers have tried to develop effective antimicrobial agents to curb the menace of pathogenic microorganisms. Such problems and needs have led to the resurgence in the use of silver-based antiseptics that may

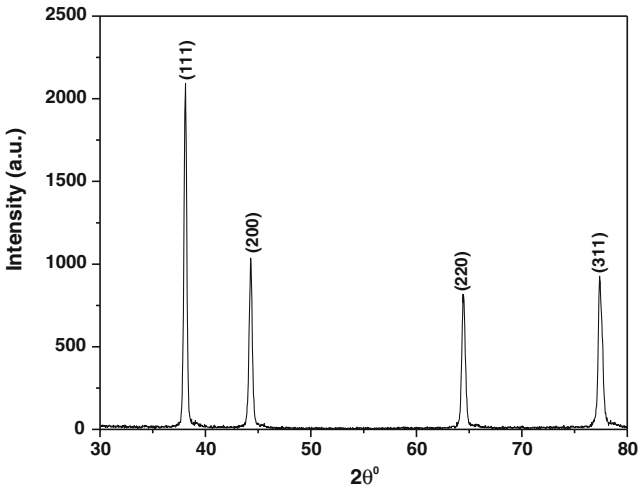

Fig. 3 XRD spectrum of silver nanowires

be linked to broad-spectrum activity and far lower propensity to induce microbial resistance than antibiotics (Kim et al. 2007). So, we have attempted to study the biological application of the as-synthesized SNWs as an antibacterial and anti-QS agent. The antibacterial activity was determined by determining the MIC which is the lowest concentrations at which a compound can inhibit a bacterium growth. A lower MIC corresponds to higher antibacterial activity. We have modified a typical MIC determination method that comprised visual inspection of broth for turbidity (bacterial growth causes a clear broth to turn turbid) and measured the inhibition by counting the number of viable cells as CFU/milliliter instead, as SNWs in MH broth gave a white turbid color in MIC tubes. As silver nanoparticles were reported to act on bacteria in a concentration-dependent manner (Kim et al. 2011), we were expecting similar results. However, non-inhibitory action of SNWs could be owing to avoidance of

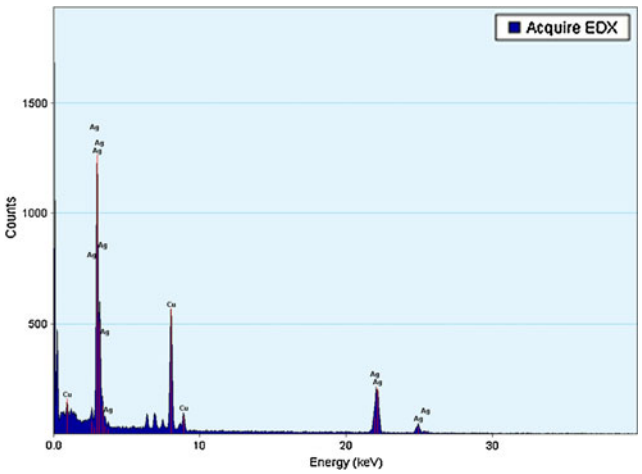

Fig. 4 Typical EDS spectrum of silver nanowires

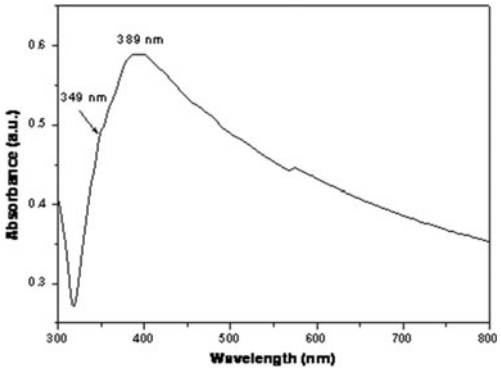

Fig. 5 UV–Vis absorption spectrum of silver nanowires

interaction of silver nanoparticles as they were stabilized by PVP. In fact, a literature search in ISI Web of Knowledge database showed that there were reports on the synthetic method of silver nanoparticles using ethylene glycol and PVP as a stabilizer (Carotenuto et al. 2000; Silvert et al. 1996; Slistan-Grijalva et al. 2005; Sun and Xia 2002); however, there was no mention on antimicrobial activity to the synthesized particles, an observation reported by us as well. So, we have decided to explore other biological application of SNWs.

Anti-quorum sensing and biofilm

As the synthesis of the violacein and biofilm are QS-mediated and controlled (Chen et al. 2011), anti-QS studies of SNWs were carried out by quantifying the synthesis of a pigment (violacein) in model organisms, *C. violaceum* and biofilm in *P. aeruginosa*, respectively. Many synthetic and natural compounds were shown as an agent that impedes the QS phenomenon in *C. violaceum* (Martinelli et al. 2004); however, *C. violaceum* has not been explored as a model organism to study the effect of nanoparticles in anti-QS studies. Our preliminary results show that, because the violacein synthesis is QS-mediated and the negative effect on violacein production in the present study was not caused by the inhibition of growth, it was clear that the SNWs were mediating the QS-controlled inhibition of violacein synthesis in *C. violaceum*. The QS-mediated inhibition of violacein is important because when the growth is not affected, there is no selective pressure for the development of resistant bacteria. Having known that SNWs is indeed an inhibitor of QS in *C. violaceum*, the possibility that it may also be able to inhibit QS-controlled phenotypes in other Gram-negative bacteria was explored. *P. aeruginosa* was chosen for this purpose because of the known QS systems that control a number of genes involved in biofilm formation and production of virulence factors (Schuster and Peter Greenberg 2006). While the molecular interplay between QS and biofilm development is still uncertain, it is clear

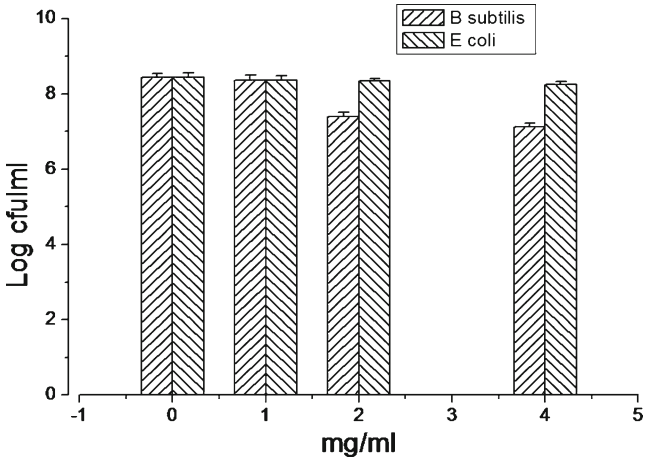

Fig. 6 A minimum bactericidal concentration of SNWs against *B. subtilis* and *E. coli*. The cultures were set up at initial inoculums of 1×10^6 in Mueller–Hinton broth containing various concentrations from (0.125–4 mg/mL) SNWs and were incubated for 12 h at 180 rpm and 37 °C. The cell number remains constant for all tested conc. *Error bars* represent the standard deviation (n=3)

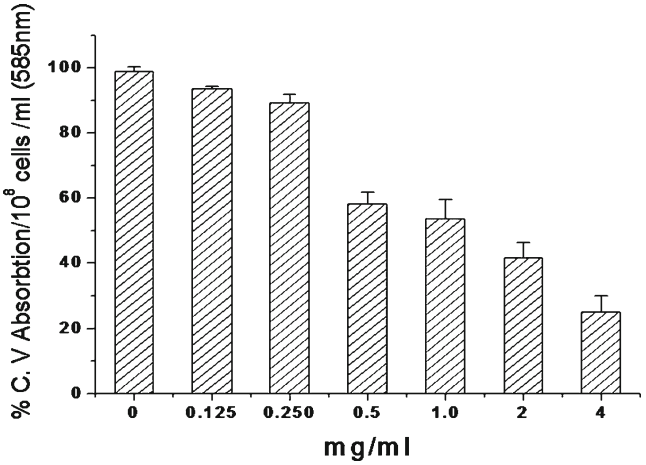

Fig. 8 Quantification of violacein pigment. The cultures of *C. violaceum* were set up at initial inoculums of 1×10^6 in Mueller–Hinton broth containing various concentrations from (0.125–4 mg/mL) SNWs and were incubated for 18 h at 180 rpm and 37 °C. Violacein quantification extracted in DMSO was read at 585 nm. At 0.5 mg/mL, there was a reduction in the synthesis of violacein by 60 % and continued till 4-mg/mL conc., after which cell death tends to start. *Error bars* represent the standard deviation (n=3)

now that QS is involved in the maturation and differentiation of biofilms (Favre-Bonté et al. 2003). A biofilm is a group of microorganisms embedded in extracellular polymeric substances that consist of polysaccharides, proteins, lipids, and nucleic acids and protects microorganism immune response and antimicrobial agents. The inhibition of QS-mediated synthesis of biofilm formation in *P. aeruginosa* was tested by growing the organism in MH broth supplemented with various concentrations of SNWs, in 24-well microtitre plates. Crystal violet retention assay was used to quantify the inhibition of biofilm formation, since crystal violet has a high affinity to the polysaccharides. The reduction in the retention of the dye at increasing concentration of SNWs is an indication of the inhibition of the biofilm (Fig. 9). The reduction was linear till 4 mg/mL, after which death of the cells commenced. In the recent year, interest in the design and synthesis of biomaterial has shifted from drug molecules to nanomaterials (Knetsch and Koole 2011; Bazaka et al. 2012), and many biomedical devices has been constructed primarily containing nanomaterials as antibiofilm agents (Monteiro et al. 2009). Silver nanoparticles and their composites have been shown to inhibit the formation of biofilm in *E. coli* (Babapour et al. 2011), *P. aeruginosa*, and *Staphylococcus epidermis* (Kalishwaralal et al. 2010). In an effort to synthesize silver nanoparticles, Babapour et al. (2011) have used silane-based matrices, phenyltriethoxysilane, containing different amounts of Ag, and showed an antibiofilm activity against *E. coli*, while biological approach was used by Kalishwarlal et al. (2010) to synthesize Ag nanoparticles (NPs) and showed an antibiofilm activity against *P. aeruginosa* and *S. epidermis*. In our study, we have used polyol approach to synthesize SNWs. Polyol approach is advantageous over the above methods of Ag NPs synthesis because the size and shape of the nanoparticles synthesized can be controlled by the controlling the reactants concentrations. Also, the biogenic method cannot be used to control the size and shape of NPs; sol-gel method also suffers from similar drawbacks. Surprisingly, the antibiofilm activity shown by Babapour et al. (2011) by using SEM seems to occur by a decrease in the number of viable cells, and less conclusive evidences were mentioned by Kalishwaralal et al.

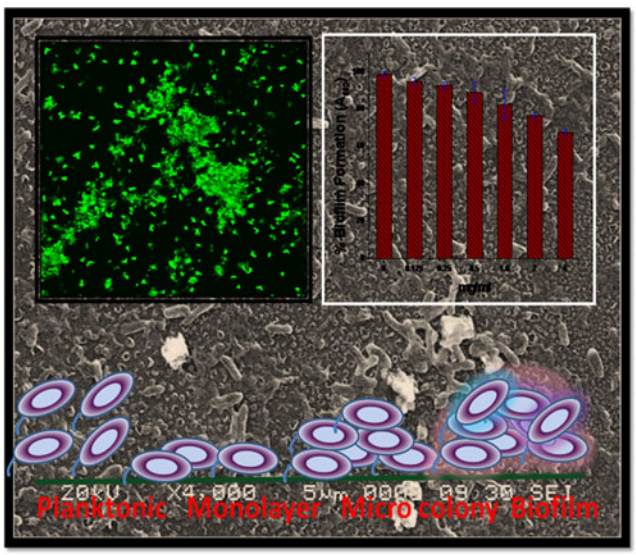

Fig. 7 Graphical representation of molecular events in QS-mediated biofilm formation/inhibition in *P. aeruginosa*

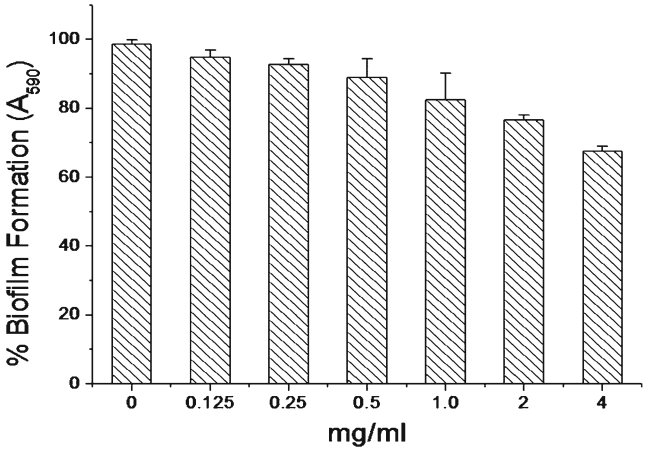

Fig. 9 Quantification of the biofilm. The cultures of *P. aeruginosa* were set up at initial inoculums of 1×10^6 in Mueller–Hinton at 37 °C. After removal of planktonic cells (culture medium), the formed biofilm was treated with 0.1 % crystal violet and extracted in acetic acid to read at 595 nm. At 4 mg/mL SNWs, there was a reduction in biofilm by 27 %. *Error bars* represent the standard deviation (n=3)

(Kalishwaralal et al. 2010) for the mentioned claim on antibiofilm activity to the biogenic silver. In our study, we report a QS-mediated inhibition of the biofilm synthesis (not by a reduction in the number of viable cells) and have used SEM and CLSM to further confirm the antibiofilm activity of SNWs. However, as the amount required to bring about the QS-mediated inhibition of violacein and biofilm formation was high, we have not carried further the experiments to further prove it. However, we have undertaken new methods to prepare and functionalize the SNWs and continue the similar studies. Under SEM, the ability of *P. aeruginosa* to form the biofilm was decreased.

This decrease cannot be because of the reduction in the number of cells as the cell density in the planktonic and biofilm were nearly same. The SEM analysis also clearly shows that the cell densities in control and test were nearly same, unlike the observation in SEM by Babapour et al. (2011), wherein a decrease in the cell densities has been shown as a measure of biofilm inhibition. The CLSM has confirmed the SEM results. As the biofilm constituent, majorly, the polysaccharides and the fact that Concanavalin A Alexa Fluor 488 has a affinity towards the mannosyl units of polysaccharides, CLSM analysis of the biofilm has showed a reduced intensity of fluorescence in the presence of SNWs, suggesting a reduction in the synthesis of a biofilm (Fig. 11). This inhibitory effect of SNWs on the biofilm may due to the presence of water channels throughout the biofilm. As in all biofilms, water channels (pores) are present for nutrient transportation; SNWs may directly diffuse through the exopolysaccharide layer through the pores and may impart antibiofilm function. However, as seen under SEM, only the outermost layer was aloofed in the presence of SNWs; it is likely that there was a diffusion limit to SNWs, possibly owing to rod

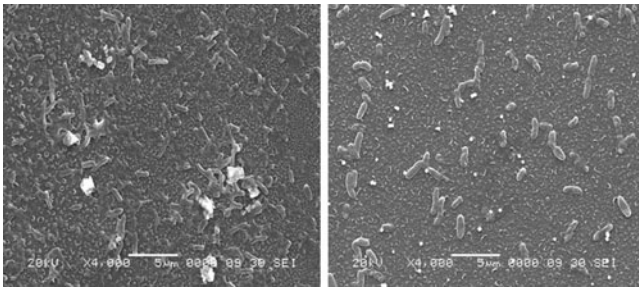

Fig. 10 Effect of SNWs on the formation of biofilm in *P. aeruginosa.* The cells of *P. aeruginosa* in the presence of SNWs (MIC_{50} value) under SEM were seen as exposed structure without the covering of polysaccharides (*right*), while in the absence of SNWs, cells were seen as embedded structures in the polysaccharide matrix (*left*). Note the similar number of cells in control and test biofilm image

shape and thus an observation as seen in Fig. 10. In a similar effort, Fabrega et al. (2009) have shown that Ag NPs potentially slough off the biofilm in a concentration-dependent manner, without decreasing the number of viable cells, an observation reported by us as well.

It is not possible to locate the precise cellular events the SNWs interrupt in the model organisms in order to be called as anti-QS agents, but it is likely that it may be acting at any stage of synthesis of diffusible signal molecules or reorganization by its cognate receptor or transduction of signal inside the cells to induce or repress the transcription of QS-regulated genes.

Thus, as-synthesized SNWs show to be a promising candidate in the inhibition of the QS. This is important because QS is a type of decision-making process used by decentralized groups to coordinate behavior. Instead of language, bacteria use signaling molecules that are released into the environment to respond quickly, coordinate their behavior, and survive. The advantage of the anti-QS approach to controlling infection is that there are few evolutionary forces that select for resistance. In other words,

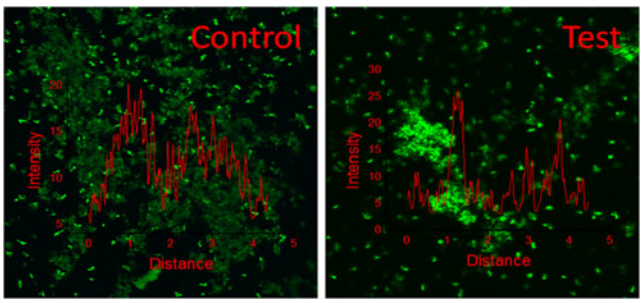

Fig. 11 Confocal image analysis of the biofilm formation in *P aeruginosa*. The cells were incubated with SNWs and stained with Concanavallin A Alexa Fluor with excitation at 488 and emission at 520 nm and observed for fluorescence. In the presence of SNWs, there was a reduction in the fluorescence, indicating a decrease in the formation of biofilm. Histogram of the intensity profile is shown as an *insert*

natural selection does not come into play, and resistant strains will unlikely to occur. Therefore, QS inhibition offers new hope in combat with multiple antibiotic-resistant bacteria. Inhibition of bacterial QS systems, rather than bactericidal or bacteriostatic strategies, may find application in many different fields, such as in medicine, agriculture, and food technology. This approach is highly attractive because it does not impose harsh selective pressure for the development of resistance with antibiotics because QS is not directly involved in processes essential for the growth of bacteria.

In summary, uniform-sized well-dispersed SNWs can be synthesized by polyol reduction route in the presence of PVP as stabilizing agent. Since these SNWs did not find an antibacterial activity and the fact the QS phenomenon is linked to the establishment of infectious diseases, a QS-mediated inhibition of biofilm in *P. aeruginosa* can be viewed as a promising method in therapeutic applications against pathogens which are increasing the development of resistance towards many antibiotics. This is important as natural selection does not come into play, and resistant strains will unlikely to occur. Thus, inhibition of bacterial QS by attenuating the signals can prevent the development of bacterial virulence and successful establishment of infections.

Acknowledgments The authors would like to thank Dr. D. P. Amalnerkar, Executive Director, C-MET, for constant encouragement throughout this work and the Department of Electronics and Information Technology (DeitY), New Delhi for the financial support. RP would like to thank UGC-SRF, and DT would like to thank DST-PURSE programme for the financial assistance.

References

Babapour A, Yang B, Bahang S, Cao W (2011) Low-temperature sol-gel-derived nanosilver-embedded silane coating as biofilm inhibitor. Nanotechnology 22:155602

Banerjee I, Pangule RC, Kane RS (2011) Antifouling coatings: recent developments in the design of surfaces that prevent fouling by proteins, bacteria, and marine organisms. Adv Mater 23:690–718

Bazaka K, Jacob MV, Crawford RJ, Ivanova EP (2012) Efficient surface modification of biomaterial to prevent biofilm formation and the attachment of microorganisms. Appl Microbiol Biotechnol 95:299–311

Blango MG, Mulvey MA (2009) Bacterial landlines: contact-dependent signaling in bacterial populations. Curr Opin Microbiol 12:177–181

Carotenuto G, Pepe GP, Nicolais L (2000) Preparation and characterization of nano-sized Ag/PVP composites for optical applications. Eur Phys J B 16:11–17

Caswell KK, Bender CM, Murphy CJ (2003) Seedless, surfactantless wet chemical synthesis of silver nanowires. Nano Lett 3:667–669

Chen D, Gao L (2004) Large-scale growth and end-to-end assembly of silver nanorods by PVP-directed polyol process. J Cryst Growth 264:216–222

Chen D, Qiao X, Qiu X, Chen J, Jiang R (2010) Convenient synthesis of silver nanowires with adjustable diameters via a solvothermal method. J Colloid Interface Sci 344:286–291

Chen G, Swem Lee R, Swem Danielle L, Stauff Devin L, O'Loughlin Colleen T, Jeffrey Philip D, Bassler Bonnie L, Hughson Frederick M (2011) A strategy for antagonizing quorum sensing. Mol Cell 42:199–209

Chen J, Wiley BJ, Xia Y (2007) One-dimensional nanostructures of metals: large-scale synthesis and some potential applications. Langmuir 23:4120–4129

Chen X, Schluesener HJ (2008) Nanosilver: a nanoproduct in medical application. Toxicol Lett 176:1–12

Davies D (2003) Understanding biofilm resistance to antibacterial agents. Nat Rev Drug Discov 2:114–122

Evans PR, Kullock R, Hendren WR, Atkinson R, Pollard RJ, Eng LM (2008) Optical transmission properties and electric field distribution of interacting 2D silver nanorod arrays. Adv Funct Mater 18:1075–1079

Fabrega J, Renshaw JC, Lead JR (2009) Interactions of silver nanoparticles with *Pseudomonas putida* biofilms. Environ Sci Technol 43:9004–9009

Favre-Bonté S, Köhler T, Van Delden C (2003) Biofilm formation by *Pseudomonas aeruginosa*: role of the C4-HSL cell-to-cell signal and inhibition by azithromycin. J Antimicrob Chemoth 52:598–604

Fievet F, Lagier JP, Blin B, Beaudoin B, Figlarz M (1989) Homogeneous and heterogeneous nucleations in the polyol process for the preparation of micron and submicron size metal particles. Solid State Ionics 32–33(Part 1):198–205

Hu JQ, Chen Q, Xie ZX, Han GB, Wang RH, Ren B, Zhang Y, Yang ZL, Tian ZQ (2004) A simple and effective route for the synthesis of crystalline silver nanorods and nanowires. Adv Funct Mater 14:183–189

Hu L, Kim HS, Lee J-Y, Peumans P, Cui Y (2010) Scalable coating and properties of transparent, flexible silver nanowire electrodes. ACS Nano 4:2955–2963

Hu X, Chan CT (2004) Photonic crystals with silver nanowires as a near-infrared superlens. App Phys Lett 85:1520–1522

Huang Y, Duan X, Cui Y, Lauhon LJ, Kim K-H, Lieber CM (2001) Logic gates and computation from assembled nanowire building blocks. Science 294:1313–1317

Kalishwaralal K, BarathManiKanth S, Pandian SRK, Deepak V, Gurunathan S (2010) Silver nanoparticles impede the biofilm formation by *Pseudomonas aeruginosa* and *Staphylococcus epidermidis*. Colloid Surfaces B 79:340–344

Kim S, Baek Y-W, An Y-J (2011) Assay-dependent effect of silver nanoparticles to *Escherichia coli* and *Bacillus subtilis*. Appl Microbiol Biotechnol 92:1045–1052

Kim JS, Kuk E, Yu KN, Kim J-H, Park SJ, Lee HJ, Kim SH, Park YK, Park YH, Hwang C-Y, Kim Y-K, Lee Y-S, Jeong DH, Cho M-H (2007) Antimicrobial effects of silver nanoparticles. Nanomed-Nanotechnol 3:95–101

Knetsch MLW, Koole LH (2011) New strategies in the development of antimicrobial coatings: the example of increasing usage of silver and silver nanoparticles. Polymer 3:340–366

Knothe H, Antal M, Krcméry V (1987) Imipenem and ceftazidime resistance in *Pseudomonas aeruginosa* and *Klebsiella pneumoniae*. J Antimicrob Chemoth 19:136–138

Lellouche J, Kahana E, Elias S, Gedanken A, Banin E (2009) Antibiofilm activity of nanosized magnesium fluoride. Biomaterials 30:5969–5978

Martinelli D, Grossmann G, Sequin U, Brandl H, Bachofen R (2004) Effects of natural and chemically synthesized furanones on quorum sensing in Chromobacterium violaceum. BMC Microbiol 4:25

Monteiro DR, Gorup LF, Takamiya AS, Ruvollo-Filho AC, Camargo ER, Barbosa DB (2009) The growing importance of materials that prevent microbial adhesion: antimicrobial effect of medical devices containing silver. Int J Antimicrob Ag 34:103–110

Murphy CJ, Gole AM, Hunyadi SE, Orendorff CJ (2006) One-dimensional colloidal gold and silver nanostructures. Inorg Chem 45:7544–7554

Peppler K, Janek J (2007) Template assisted solid state electrochemical growth of silver micro- and nanowires. J Electrochim Acta 53:319–323

Rai MK, Deshmukh SD, Ingle AP, Gade AK (2012) Silver nanoparticles: the powerful nanoweapon against multidrug-resistant bacteria. J Appl Microbiol 112:841–852

Rana D, Matsuura T (2010) Surface modifications for antifouling membranes. Chem Rev 110:2448–2471

Reading NC, Sperandio V (2006) Quorum sensing: the many languages of bacteria Fems. Microbiol Lett 254:1–11

Salata O (2004) Applications of nanoparticles in biology and medicine. J Nanobiotechnology 2:3

Sancia R, Volkan M (2009) Surface-enhanced Raman scattering (SERS) studies on silver nanorod substrates. Sensor Actuat B-Chem 139:150–155

Schuster M, Peter Greenberg E (2006) A network of networks: quorum-sensing gene regulation in *Pseudomonas aeruginosa*. Int J Med Microbiol 296:73–81

Shen Q, Sun J, Wei H, Zhou Y, Su Y, Wang D (2007) Fabrication of silver nanorods controlled by a segmented copolymer. J Phys Chem C 111:13673–13678

Silvert P-Y, Herrera-Urbina R, Duvauchelle N, Vijayakrishnan V, Elhsissen KT (1996) Preparation of colloidal silver dispersions by the polyol process. Part 1-Synthesis and characterization. J Mater Chem 6:573–577

Slistan-Grijalva A, Herrera-Urbina R, Rivas-Silva JF, Ávalos-Borja M, Castillón-Barraza FF, Posada-Amarillas A (2005) Assessment of growth of silver nanoparticles synthesized from an ethylene glycol–silver nitrate–polyvinylpyrrolidone solution. Physica E 25:438–448

Suman KB, Andrew TF, Rahul VK (2009) A model for signal transduction during quorum sensing in *Vibrio harveyi*. Phys Biol 6:046008

Sun Y, Xia Y (2002) Shape-controlled synthesis of gold and silver nanoparticles. Science 298:2176–2179

Tamboli MS, Kulkarni MV, Patil RH, Gade WN, Navale SC, Kale BB (2012) Nanowires of silver–polyaniline nanocomposite synthesized via in situ polymerization and its novel functionality as an antibacterial agent. Colloid Surfaces B 92:35–41

Tian X, Li J, Pan S (2009) Facile synthesis of single-crystal silver nanowires through a tannin-reduction process. J Naopart Res 11:1839–1844

Wang Z, Liu J, Chen X, Wan J, Qian Y (2005) A simple hydrothermal route to large-scale synthesis of uniform silver nanowires. Chem Eur J 11:160–163

Whitehead NA, Barnard AM, Slater H, Simpson NJ, Salmond GP (2001) Quorumsensing in Gram-negative bacteria. FEMS Microbiol Rev 25:365–404

Wiley B, Sun Y, Mayers B, Xia Y (2005) Shape-controlled synthesis of metal nanostructures: the case of silver. Chem Eur J 11:454–463

Xia Y, Yang P, Sun Y, Wu Y, Mayers B, Gates B, Yin Y, Kim F, Yan H (2003) One-dimensional nanostructures: synthesis, characterization and applications. Adv Mater 15:353–389

Yang G-W, Li H (2008) Sonochemical synthesis of highly monodispersed and size controllable Ag nanoparticles in ethanol solution. Mater Lett 62:2189–2191

You T, Xu S, Sun S, Song X (2009) Controllable synthesis of pentagonal silver nanowires via a simple alcohol-thermal method. Mater Lett 63:920–922

Zhai T, Fang X, Liao M, Xu X, Zeng H, Yoshio B, Golberg D (2009) A comprehensive review of one-dimensional metal-oxide nanostructure photodetectors. Sensors 9:6504–6529

Zhu YP, Wang XK, Guo WL, Wang JG, Wang C (2010) Sonochemical synthesis of silver nanorods by reduction of sliver nitrate in aqueous solution. Ultrason Sonochem 17:675–679

Zou K, Zhang XH, Duan XF, Meng XM, Wu SK (2004) Seed-mediated synthesis of silver nanostructures and polymer/silver nanocables by UV irradiation. J Cryst Growth 273:285–291